Thermal relaxation of magnetic clusters in amorphous $Hf_{57}Fe_{43}$ alloy

2007 J. Phys.: Condens. Matter 19 296207

(http://iopscience.iop.org/0953-8984/19/29/296207)

IOP PUBLISHING JOURNAL OF PHYSICS: CONDENSED MATTER

J. Phys.: Condens. Matter **19** (2007) 296207 (16pp) doi:10.1088/0953-8984/19/29/296207

Thermal relaxation of magnetic clusters in amorphous $Hf_{57}Fe_{43}$ alloy

Damir Pajić[1,4], Krešo Zadro[1], Ramir Ristić[2], Ivica Živković[3], Željko Skoko[1] and Emil Babić[1]

[1] Department of Physics, Faculty of Science, University of Zagreb, Bijenička cesta 32, HR-10000 Zagreb, Croatia
[2] Department of Physics, University of Osijek, Trg Ljudevita Gaja 6, HR-31000 Osijek, Croatia
[3] Institute of Physics, Bijenička cesta 46, HR-10000 Zagreb, Croatia

E-mail: dpajic@phy.hr

Received 27 March 2007, in final form 15 June 2007
Published 5 July 2007
Online at stacks.iop.org/JPhysCM/19/296207

Abstract

The magnetization processes in binary magnetic/non-magnetic amorphous alloy $Hf_{57}Fe_{43}$ are investigated by the detailed measurement of magnetic hysteresis loops, temperature dependence of magnetization, relaxation of magnetization and magnetic ac susceptibility, including a nonlinear term. Blocking of magnetic moments at lower temperatures is accompanied by the slow relaxation of magnetization and magnetic hysteresis loops. All of the observed properties are explained by the superparamagnetic behaviour of the single domain magnetic clusters inside the non-magnetic host, their blocking by the anisotropy barriers and thermal fluctuation over the barriers accompanied by relaxation of magnetization. From magnetic viscosity analysis based on thermal relaxation over the anisotropy barriers it is found that magnetic clusters occupy the characteristic volume from 25 up to 200 nm^3. The validity of the superparamagnetic model of $Hf_{57}Fe_{43}$ is based on the concentration of iron in the $Hf_{100-x}Fe_x$ system that is just below the threshold for long range magnetic ordering. This work also throws more light on the magnetic behaviour of other amorphous alloys.

1. Introduction

Magnetism in nanostructured materials has been a very popular topic and a subject of intense research for many years [1]. Magnetic colloids [2] and nanometre sized magnetic objects, have been a subject of interest for quite some time. Now, a large impact of nanoparticulate and nanostructured magnetic materials can be seen in many products as well as in high-tech devices.

[4] Author to whom any correspondence should be addressed.

0953-8984/07/296207+16$30.00

In addition to use in commercial applications, nanostructured magnetic materials show a broad spectrum of fundamental physical phenomena which became accessible with development of the synthesis and characterization of nanomagnets.

When talking about magnetic particles of a size below about 100 nm, superparamagnetism [3] is an usual keyword. It has been shown theoretically that for particles of these sizes it is favourable to be single domain [4], and this has also been measured in magnetic colloid [5]. The giant magnetic moments of these particles fluctuate over the anisotropy barrier according to the activation law [6]. At low temperatures this fluctuation becomes slower than the measurement of one point, resulting in a very rich phenomenology of non-equilibrium systems and slow relaxation of their magnetization.

In magnetic alloys it is possible that (ferro)magnetic single-domain clusters are formed within a non-magnetic or a much weaker magnetic matrix [7]. The alloy exhibits a long range ferromagnetic ordering for a high concentration of magnetic atoms, whereas for low concentrations of magnetic atom it exhibits paramagnetic behaviour, and somewhere between it is superparamagnetic. Modelling and computational simulation of processes in alloys is very realistic and the experimental magnetic results are reproduced very well [8], which helps to establish a connection between the microscopic picture and macroscopic properties.

Magnetic ordering in the binary $Hf_{100-x}Fe_x$ system was studied previously for a different iron concentration x [9, 10]. For $x \geqslant 50$ the long range magnetic order was observed [9] with critical temperatures up to 300 K. For $x \leqslant 40$ the system is paramagnetic with increasing Curie constant as x increases [10]. After the observation of splitting between the zero-field-cooled and field-cooled magnetization curves and slow relaxation of magnetization, together with hysteresis curves at low temperatures [11], a detailed magnetic investigation of $Hf_{57}Fe_{43}$ amorphous alloy was undertaken. In this paper the results will be presented and explained within the framework of superparamagnetism of magnetic clusters, their blocking by the anisotropy barriers and thermal fluctuation over the barriers accompanied by relaxation of magnetization.

2. Experimental procedure

The investigated binary magnetic/non-magnetic amorphous alloy $Hf_{57}Fe_{43}$ within the Hf–Fe system was prepared using a melt-spinning method. Starting elements were precisely weighed to fulfil the desired molar proportions and after the whole process the total mass did not change. Melting in the argon atmosphere was performed many times in order to obtain a compositionally homogeneous alloy.

X-ray diffraction (XRD) patterns were taken at room temperature using an automatic Philips diffractometer, model PW1820 (Cu Kα radiation, graphite monochromator, proportional counter), in Bragg–Brentano geometry. The diffraction intensity was measured in the angular range $20° \leqslant 2\theta \leqslant 80°$.

Magnetic measurements were performed using a Quantum Design MPMS5 SQUID magnetometer, which uses the extraction method to measure the magnetic moment of the sample with a very high accuracy. Due to the high stability of temperature and the stable homogeneous magnetic field, this equipment is very suitable for long-lasting magnetic relaxation measurements.

The dependence of the magnetic moment of the sample m on the temperature T is measured using two modes: zero-field-cooled (ZFC) and field-cooled (FC), both of them during the increase of T. The temperature below which the splitting of ZFC and FC curves appears is called the blocking temperature T_B. It is important to mention that there are two different definitions of T_B with slightly different values: the temperature at which the ZFC curve attains

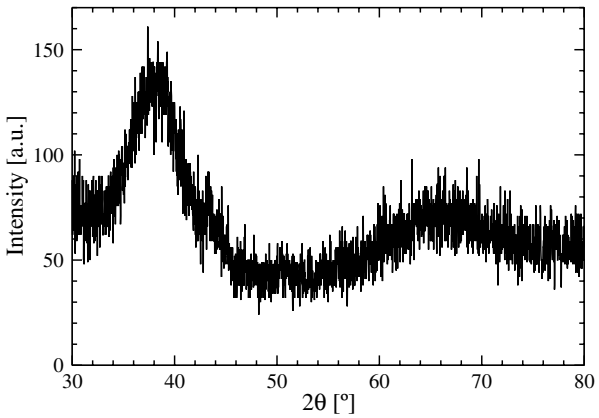

Figure 1. XRD pattern of the as-quenched $Hf_{57}Fe_{43}$ sample.

a maximum (T_{max}) or the temperature below which the splitting appears (T_{irr}), both having a reasonable interpretation.

The $m(H)$ curves for the applied magnetic field $\mu_0 H$ up to 5.5 T at different stable temperatures were measured. Hysteresis loops were measured with a maximum applied field of 0.2 T because all the curves are reversible above this field.

Very detailed and precise measurement of the relaxation of the magnetic moment of the sample for a broad range of stable temperatures from 1.8 up to 25 K was performed. The sample was at first heated to 100 K, well above T_B in zero applied magnetic field. Then a magnetic field of 0.01 T was imposed. After some waiting time the sample was cooled down to the desired temperature and stabilized. Finally, the magnetic field was reversed to the opposite direction (from 0.01 to −0.01 T) and m was measured as the time elapsed over ∼3 h. This procedure was repeated for many different target temperatures below T_B with very high reproducibility.

The AC susceptibility measurements were performed using the commercial CryoBIND system. The first and the third harmonics were measured simultaneously with two lock-in amplifiers connected in parallel. The amplitude and the frequency of the driving field were set to 1 mT and 990 Hz, respectively.

3. Results of measurements

In order to check the structure, the XRD patterns of the as-quenched $Hf_{57}Fe_{43}$ samples were taken and the result is shown in figure 1. No crystallite peak was detected, but two extremely broad maxima centred at 2θ of 39° and 66° were observed, thus indicating that the alloy was in a completely amorphous state. The XRD measurements were done by exposing both as-quenched ribbon surfaces to the x-ray beam—the surface of the ribbon which was in contact with the inert atmosphere and the surface which was in contact with the wheel. This was done to find out whether there was any difference in the crystal structure between the two surfaces, which could be due to different treatments being applied to each surface. The XRD patterns were similar, thus showing the amorphous nature of both sides of the ribbon. Positions of these broad maxima correspond to the results presented in [12] for a similar Hf–Fe system.

The temperature dependence of magnetization $M(T)$ is measured in ZFC and FC modes for several temperatures and some of them are shown in figure 2. The well-pronounced ZFC–FC splitting points to the blocking of the magnetic moment of the sample below T_B. It has been observed that T_B decreases as the applied magnetic field H increases.

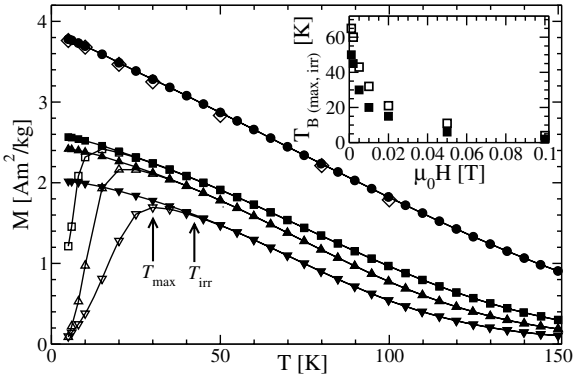

Figure 2. Zero-field-cooled (ZFC, hollow symbols) and field-cooled (FC, full symbols) $M(T)$ curves in different applied magnetic fields $\mu_0 H$: 0.005 T (▼), 0.01 T (▲), 0.02 T (■), 0.1 T (●) and from $M(H)$ curves (◇); lines are guides to the eye. The inset shoes the dependence of blocking temperatures T_{max}(■) and T_{irr}(□) on applied magnetic field $\mu_0 H$.

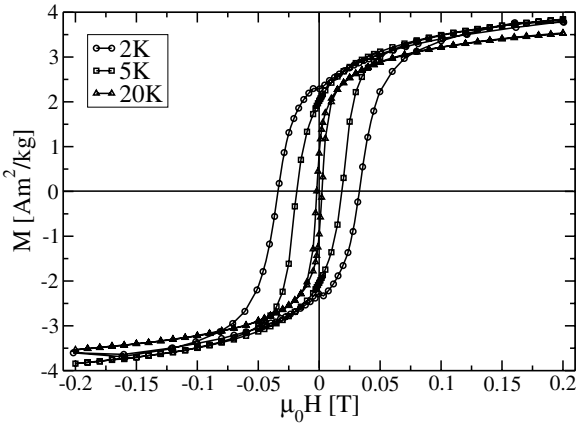

Figure 3. Magnetic hysteresis loops $M(H)$ at some temperatures with maximum applied field of 0.2 T. Lines are guides to the eye.

Some of measured hysteresis loops of the sample are presented in figure 3. They get narrower as the temperature increases, becoming almost reversible above approximately 30 K. Obviously, the irreversibility is destroyed by thermal effects. For all measured temperatures the irreversibility appears below a field of 0.14 T, so that the maximum field of 0.2 T was high enough to study the hysteretic properties.

Presented hysteresis loops are still far from saturation. $M(H)$ dependence is measured up to a maximum possible field of 5.5 T for different temperatures and is plotted in figure 4. The saturation magnetization is still unreachable at 5.5 T and the lack of H/T scaling tells us that the pure Curie–Brillouin–Langevin approach is not applicable. The $M(H)$ dependence is nonlinear even for small magnetic fields of 0.002 T and up to room temperature. The documented paramagnetic susceptibility of hafnium is 0.42×10^{-2} J T^{-2} kg^{-1} at room temperature with a weak temperature dependence (0.4×10^{-2} J T^{-2} kg^{-1} at 77 K and 0.46×10^{-2} J T^{-2} kg^{-1} at 4.2 K) [13]. Recalculated, this amounts to only ≈0.5% of mass magnetization in our sample at 100 K and 5.5 T, (unjustifiably) assuming it to be an independent additive contribution.

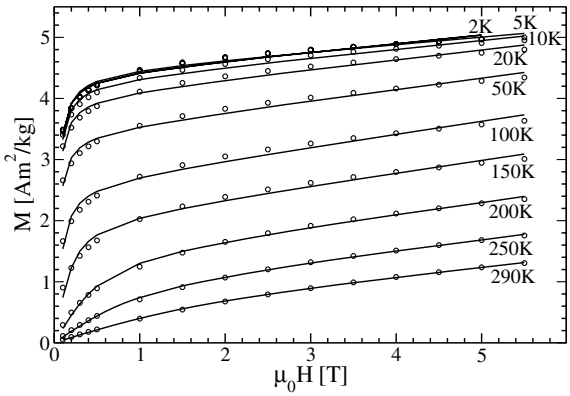

Figure 4. Dependence of magnetization M of the sample on applied magnetic field H for different temperatures. Lines are fitted functions (see equation (5) and figure 9).

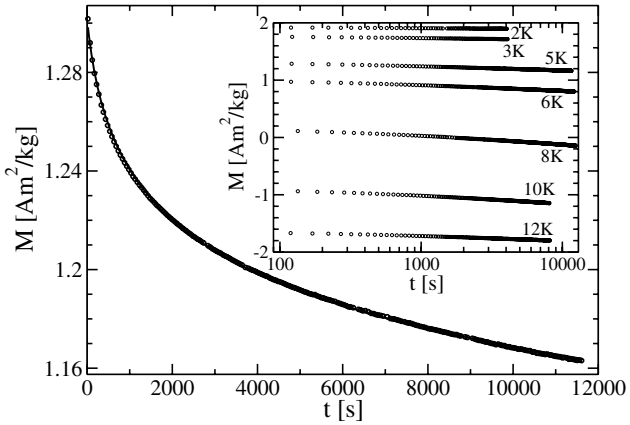

Figure 5. Relaxation of magnetization at 5 K with a logarithmic fitting curve. Inset: relaxation of magnetization at some temperatures on a logarithmic timescale.

The blocking of magnetic moments below T_B results in the slow and measurable relaxation of magnetization presented in figure 5 for some of the measured temperatures. All of measured relaxation data for more than 40 different temperatures between 1.8 and 25 K are logarithmic in time.

The AC susceptibility has been recognized as a powerful tool for investigating the properties of systems which show superparamagnetic and/or glassy behaviour. In particular, the measurements of the third harmonic (χ_3) have been used to differentiate between these two systems which show very similar behaviour in the first harmonic (χ_1) [14]. It has been theoretically predicted that a spin-glass system should show a divergence of the third harmonic [15] at the transition temperature T_g; this has been confirmed experimentally [14, 16]. On the other hand, superparamagnetic systems show a non-diverging peak in χ_3 around the blocking temperature T_B with a T^{-3} dependence above T_B [14, 17], in accordance with Wohlfarth's blocking model [18]. In figure 6 we present the results of the measurements of the first and the third harmonic of the AC susceptibility as a function of temperature. χ_1 shows a round maximum at 66 K and a monotonic decrease at higher temperatures. χ_3 is zero below

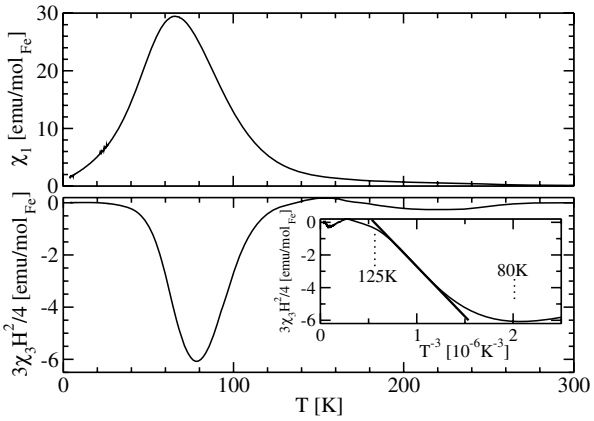

Figure 6. Temperature dependence of linear magnetic susceptibility χ_1 (up) and nonlinear susceptibility χ_3 transformed to $4/3 \cdot \chi_3 H^2$ (down) measured at 1 mT and 990 Hz. The inset shows the dependence of nonlinear susceptibility on T^{-3}.

20 K, shows a minimum at 79 K, a small broad feature centred around 220 K and eventually goes to zero for $T > 300$ K.

Analysis of the temperature dependence of χ_3 around the relatively broad minimum showed non-diverging behaviour, excluding the possibility that a spin-glass order is present in $Hf_{57}Fe_{43}$. In the inset we show the χ_3 versus T^{-3} dependence, predicted to be a straight line in the case of superparamagnets [18]. The range in which a linear behaviour is observed is rather small ($\sim$10 K). Recently, a similarly small interval has been observed in the $Li_{0.5}Ni_{0.5}O$ system [17] and was attributed to a small difference between the blocking temperature T_B and the intra-particle spin-correlation temperature, which is much larger in conventional superparamagnetic systems. Also, it is possible that the deviation from linearity comes from the superposition of susceptibilities of superparamagnetic clusters which have different blocking temperatures.

The small broad feature in the $\chi_3(T)$ graph is located around 220 K. We observe that neither χ_1 nor magnetization show visible deviations in that temperature range so we believe that it does not influence the main results presented in this paper. We will address this question in the future.

4. Analysis and discussion

The performed magnetic characterization alone gives many useful details about magnetic properties and processes in amorphous $Hf_{57}Fe_{43}$ magnetic alloy. In general, there is a lack of precise physical models of such kinds of magnetic alloys and the descriptions are more phenomenological. Results presented in section 3 fit very well within the frame of thermal activation of blocked magnetic moments of superparamagnetic clusters, which is assisted by the applied magnetic field. Now, different parameters derived from the presented raw data will be analysed within this frame in the context of some existing models.

4.1. Blocking of magnetization

Taking as the origin of blocking the magnetic anisotropy barrier of height U, the relaxation time τ of the magnetic moment of the particle/cluster at temperature T is determined by the

activation law [6, 19]

$$\tau = \tau_0 \exp(U/k_B T) \tag{1}$$

where τ_0 is of the order 10^{-9}–10^{-11} s [19]. At $T = T_B$ the relaxation time becomes equal to the time of measurement of one point $\tau = \tau_{exp}$, which is about 100 s in our experiment. Using the blocking temperature for an applied magnetic field of 0.01 T of $T_{max} = 20$ K and $T_{irr} = 30$ K and taking (1) it follows that $U \approx 27\ k_B T_{max} = 7.3 \times 10^{-21}$ J and $U \approx 27\ k_B T_{irr} = 1.1 \times 10^{-20}$ J, corresponding to barrier heights responsible for blocking of moments below 20 K and 30 K, respectively, in a magnetic field of 0.01 T. We take $\tau_0 = 10^{-10}$ s [19], knowing that there are many difficulties [20], but fortunately the estimation of barrier height does not depend significantly on the chosen values for τ and τ_0.

In an applied magnetic field H the barrier height which prevents the escape of magnetic moment is reduced as $U = KV(1 - \mu H/2KV)^2$, where K is the anisotropy energy density, V is the volume of the cluster and μ is magnetic moment of the cluster. In our case there is no reason for clusters to be of a single size and have unique barrier heights, nor for them to be equally oriented. Therefore, $T_B(H) = (KV)/[k_B \ln(\tau_{exp}/\tau_0)][1 - (\mu H)/(2KV)]^2$ derived for an ensemble of single sized equally oriented nanoparticles [3] is not expected to fit the extracted $T_{max,irr}(H)$ dependence. On the contrary, it is known to describe correctly the blocking temperature in the single-molecule magnet Mn_{12}-acetate [21], where all magnetic units are equal.

Also, the measured $T_B(H)$ cannot be described by $H^{-2/3}$ nor any other similar power law dependence that is characteristic for some spin-glass and/or superparamagnetic systems [22]. Pure exponentials are not suitable either. However, the measured FC curve with a broad peak is not characteristic for spin-glass behaviour [23] but corresponds more likely to distributed blocked superparamagnetic clusters.

For measurement in a field of 0.1 T there is no ZFC–FC splitting down to the lowest measured temperature of 5 K, consistent with hysteresis loops from figure 3. Also, it is shown in figure 2 that the ZFC and FC values of magnetization for 0.1 T are equal to the values taken from the hysteresis curves. This overlap says that in the case where the applied field destroys the irreversibility, the history of the magnetizing process plays no role.

4.2. Magnetic hysteresis

The question about the origin of the magnetic hysteresis in amorphous $Hf_{57}Fe_{43}$ is to be answered by looking at the slow relaxation of superparamagnetic units, indicated by the results presented above. The lowering of T_B with increasing magnetic field illuminates the origin of hysteretic irreversibility: the applied magnetic field changes the barriers established by anisotropy and helps the magnetic moments to overcome the barriers, so that the system should be at a lower temperature in order that the higher number of clusters stays on the same side of the barrier for a considerable amount of time. From the other side, increasing the temperature makes the loops narrower (figure 3), indicating that the field needed to overcome the barrier is smaller because the moments already have a higher thermal energy. The mechanism of magnetic hysteresis in the case of heterogeneous alloys was analysed precisely by Stoner and Wohlfarth [24], but without any reference to temperature dependent dynamics.

The measured temperature dependence of the coercive field H_c is shown in figure 7. The data are fitted very well by the exponential function $H_c(T) = H_{c0} \exp(-\alpha T)$. The best agreement is achieved for $\mu_0 H_{c0} = 0.0455$ T and $\alpha = 0.158$ K^{-1}.

When the applied field H is high enough to decrease the previously discussed energy barriers to $\approx 25 k_B T$, the reversal process can be thermally activated within the time of one

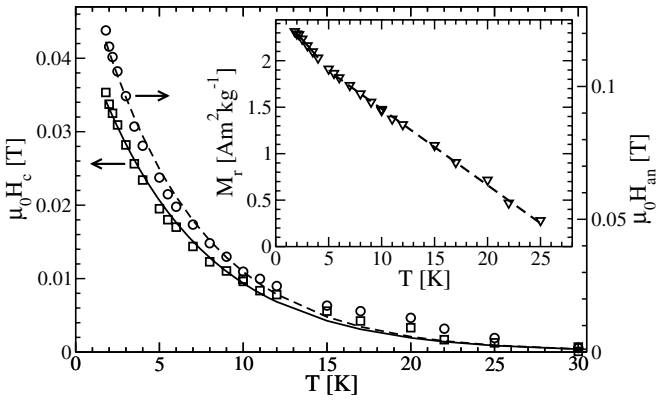

Figure 7. Temperature dependence of coercive field H_c (□), anisotropy field H_{an} (○) and remanent magnetization M_r (▽). Lines represent fitting curves.

measurement [3]. The lack of the consequently proposed dependence $H_c = 2\ \mathrm{K\,V}/\mu\{1 - [(k_B T \ln(\tau_{exp}/\tau_0))/(KV)]^{1/2}\}$ in describing the data shows again that the anisotropy barriers in our ensemble of magnetic clusters are not uniform.

The exponential dependence $H_c(T)$ describes very well the behaviour in other different systems. In a magnetic garnet film the coercivity was connected to the temperature dependence of anisotropy and a simple exponential model was an ideal fit [25]. The rare-earth–transition-metal random magnet (FeSm) exhibits also this kind of $H_c(T)$ dependence [26]. In such systems characterized by strong ferromagnetic exchange and random magnetic anisotropy the atomic magnetic moments are correlated on a small scale, while on a large scale the magnetization rotates stochastically through the sample. There $H_c(T)$ is exponential for different exchange and anisotropy values [27]. Exponential dependence was observed in FeZr amorphous alloy, $Dy_{60}Fe_{40}$, $(Gd_{1-x}Tb_x)_2Cu$, and also in many simulations and theoretical calculations [28].

In $Hf_{57}Fe_{43}$, an exponential dependence appears because of the coercive field, reflecting the difficulty of reversing the whole system of magnetic clusters which change the orientation of their magnetic moments over the anisotropy energy barriers by thermal relaxation. Our value of α is half of the value obtained in the random anisotropy model [27] where the coercivity was investigated for a limited range of the anisotropy to exchange ratio and a decrease of α with decreasing exchange ratio was observed. According to that study, our value of α points to negligible exchange interaction between the units. The most complete simulation of coercivity in a single-domain particle system [29] includes the contributions from distributed blocked particles and superparamagnetic particles. Accordingly, our results point to the relatively broad distribution of cluster sizes. Additionally, with a power law predicted for the disordered spins on nanoparticle surfaces [30] and randomly oriented particles under the thermal influence [31], it is not possible to fit the data.

The temperature dependence of remanence in random anisotropy model was found to be exponential too [32]. In our measurements $M_r(T)$ is linear in two regions (shown in figure 7). At lower temperatures (below 5 K) the change of remanence with temperature is $-0.132\ \mathrm{Am^2\,kg^{-1}\,K^{-1}}$, at higher temperatures (5–25 K) it is $-0.082\ \mathrm{Am^2\,kg^{-1}\,K^{-1}}$, and above 25 K the remanence fluctuates at small values. Here, a slower decrease happens for a longer duration of hysteresis loop measurement. This qualitative correlation is reflected in the design of the experiment where the measurement was performed faster below 4.2 K

(liquid helium). Generally, the memory related to remanence lasts longer with lower temperature. It is reasonable that the system memorizes the state more intensively when the change of the applied field is faster, because the system has no time to come closer to the new equilibrium. Altogether, a slower change of remanence is observed when the change of field is slower, due to the lower ability of memory alone. This explanation fits very well within the frame of dynamical hysteresis caused by thermal activation over the anisotropy barrier. A linear dependence of remanent magnetization on temperature was found in a simulation of magnetic processes in amorphous alloy with nanometre sized magnetic clusters having a random distribution of orientation [33]. This is also applicable for a random distribution of sizes, including in our system.

The anisotropy field H_{an} depends on temperature, as shown in figure 7. H_{an} is obtained from hysteresis loops as the field above which the loops become reversible. This is reasonable in systems where the anisotropy axes are distributed in all directions, which is expected for our amorphous material. The clusters having perpendicularly oriented anisotropy axes with respect to magnetic field contribute weakly to the hysteretic irreversibility, but the clusters with axis oriented in the direction of applied magnetic field define the highest field at which irreversibility exists. Again, the exponential function $H_{an}(T) = H_{an0}\exp(-\beta T)$ (like in [25]) was applied giving the parameters $\mu_0 H_{an0} = 0.157$ T and $\beta = 0.165$ K^{-1}. The slight departure of the anisotropy field data from the exponential curve at temperatures above 15 K, as well as for coercive field data, may be caused by a small number of large clusters or by a very weak interaction between clusters which contribute with narrow hysteresis loops.

The measured ratio $H_c/H_{an} \approx 0.3$ in the temperature interval 2–20 K (it decreases slightly above 20 K) is in agreement with a value obtained for a system of randomly oriented single domain particles with a relatively broad distribution over sizes [34].

Lowering of H_c, M_r and H_{an} with increasing temperature appears because the system has more and more energy to turn the moments of the clusters over the barriers, so that the smaller the magnetic field needed to reverse the direction of magnetization, the less able the system is to keep the moments blocked and a lower field is needed to make the system reversible.

4.3. Relaxation of magnetization

After the change of direction of applied magnetic field the system goes very quickly to the initial value of magnetization. This part of the fast magnetic relaxation is not measurable using our experimental device which has a time resolution of ∼1 min. From an initial value which depends on temperature, the sample is relaxing slowly toward the equilibrium determined by magnetic field and temperature, which is practically close to the ZFC value of magnetization. When plotted with a logarithmic timescale, all the relaxation curves appear linear and the measured relaxation data were fitted very precisely by

$$M(t) = M_0 - S\ln(t - t_0). \tag{2}$$

S is called the magnetic viscosity or logarithmic relaxation rate, M_0 is the initial magnetization and t_0 has the meaning of time from which the system started to relax slowly. The fitting results for S at different temperatures are shown in figure 8. On its lower temperature part $S(T)$ reflects the increase of the relaxation rate with temperature. Contrarily, the decrease of S at $T > 9$ K in accordance with the magnetic moment blocking hypothesis does not mean that the relaxation becomes slower, but just that a small number of moments remain to relax after the main part of the sample has been relaxed prior to taking any measurement at this temperature. Parameter $-t_0$ is mainly between 100 and 200 s for all temperatures, which is somewhere during the superconducting coil recharging time and is consistent with the assumed fast arrival to the initial magnetization before the measurement.

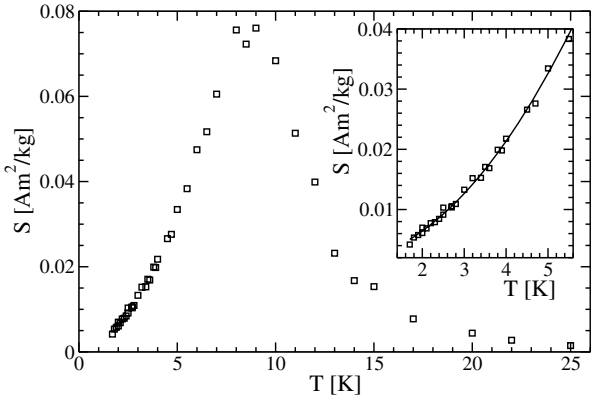

Figure 8. Temperature dependence of magnetic viscosity S of the sample. Inset: low temperature region with a regression curve.

Some microscopic results can be obtained when interpreting that data in the model of activation over barriers. The logarithmic relaxation of magnetization in the ensemble of superparamagnetic units was derived using the notion of critical barrier height [35]. An ensemble of magnetic entities consists of characteristic magnetic moment units with corresponding energy barriers. From the already discussed activation law (1) it follows that in the distribution of energy barriers there is a critical one, above which the moment of the cluster is stable on the timescale of the relaxation measurements. The clusters with lower barriers relaxed to their equilibrium determined by the applied magnetic field $H < 0$ prior to taking the measurement. The clusters with higher barriers remain blocked in the original state determined by the cooling field $H > 0$. As time passes, some additional moments jump over the barrier and the magnetization progresses toward the new equilibrium determined by the applied field. Because of the impossibility of covering the whole range of exponentially distributed relaxation times with the measurement at one temperature within the finite time, it is necessary to look at just the limited time interval, which is very narrow compared to the timescale covered by relaxations over all available barrier heights. By changing the temperature at which the relaxation is measured, we cover different barrier heights probed during the experimental time-window. A similar approach was applied in [36].

We are aware that the cutting of overparametrization inside the logarithmic function leads to a problem with units, but it is useful if carefully interpreted. There is also an approach with another functional dependence on time [37], which shows that because of slow relaxation distributed over many time decades it is possible to use a small time-window of many functions. Despite the objections against the use of a logarithmic fit [37], it has turned out to be successful in other cases [38, 39], so we used it.

Likewise, starting from the exponential relaxation of magnetic nanoparticles in an ensemble with distributed size a slightly different form of magnetic viscosity is presented in [19]. For low temperature magnetic viscosity $S \propto T^2$ was found. The addition of a constant term in $S = aT^2 + b$ was necessary in order to fit our low temperature data in figure 8 for $T \leqslant 5.5$ K resulting in $a = 0.001\,24$ au and $b = 0.001\,45$ au. Finite b would eventually point to the possibility of quantum tunnelling of magnetization, but for this claim lower temperatures should be investigated. In $Cu_xFe_{3-x}O_4$ nanoparticles [40] and many other systems, $S(T)$ was found to be linear and tunnelling would be manifest as a plateau in $S(T)$ [41].

To extract the barrier heights from figure 8 a link between temperature and barrier height is needed. Using for τ in (1) the characteristic duration of the relaxation experiment $\tau \sim 1000$ s it follows that $U \approx 30k_BT$. A maximum of S is achieved at $T = 8.5$ K, corresponding to $U = 3.5 \times 10^{-21}$ J. This is the barrier height for the clusters with the highest magnetization contribution in the whole system. Above this value S decreases abruptly up to $U = 7 \times 10^{-21}$ J, showing that the number of magnetic clusters with higher barriers decreases abruptly too. Eventually, there is a small number of clusters with higher barriers, up to $U = 10^{-20}$ J, and still higher barriers were not probed by our experiment. The lowest measured temperature in $S(T)$ corresponds to $U = 7.4 \times 10^{-22}$ J. Lower barriers were not probed.

Blocking temperature T_{max} from figure 2 corresponds to the highest significant contribution in the $S(T)$ dependence from figure 8, making it the temperature at which almost all of the clusters have already relaxed to the equilibrium. On the other hand T_{irr} corresponds to the value on this plot to which a further small decrease in $S(T)$ is observed. This slight decrease amounts to a small number of bigger moments which are stable for much longer than the timescale of experiment. Such a shape of $S(T)$ is the reason for $T_{max} < T_{irr}$. Also, the shape of $S(T)$ means that the spin-glass possibility can be excluded as a cooperative random freezing. The ZFC curve starts to decrease broadly above T_{max} because of fast fluctuations of the magnetization of smallest clusters, and at T_{irr} when nearly all clusters are relaxed it meets the FC curve (figure 2). So, the consistency between the magnetic viscosity and blocking temperatures is shown.

4.4. Magnetic cluster sizes

Magnetic cluster sizes can be obtained from barrier height data if the magnetic anisotropy density K is known. K is approximately calculated from hysteresis loops using

$$K = \mu_0 H_{an} M_s/2 \tag{3}$$

according to the well-known magnetic anisotropy models [19, 24, 39]. The dependence of the anisotropy field H_{an} on temperature is shown in figure 7. The extrapolation to zero temperature is taken from the fit in order to exclude the thermal effects on anisotropy: $\mu_0 H_{an0} = 0.157$ T. The saturation magnetization M_s is extracted from the high field magnetization variation. The data above 2 T of the $M(H)$ curve for the lowest measured temperature of 2 K are fitted with the usual expression

$$M = M_s\left(1 - \frac{4K^2}{15M_s^2H^2}\right) + \chi_m H \tag{4}$$

based on a model from [42]. The paramagnetic susceptibility χ_m of the matrix becomes somewhat bigger than χ_{Hf} when it is appropriately scaled, taking the mass contribution $w(\mathrm{Hf}) = 0.819$. From the obtained $M_s = 4.6$ Am^2 kg^{-1} and the mass density of $Hf_{57}Fe_{43}$ $\rho \approx 1.2 \times 10^4$ kg m^{-3} [43][5], and the volume saturation magnetization is $M_s^V = 5.6 \times 10^4$ A m^{-1}. This should be divided by the iron mass contribution $w(\mathrm{Fe}) = 0.191$ because the paramagnetism of hafnium is much weaker than the contribution of iron. It follows that $K = 2.1 \times 10^4$ J m^{-3}. The same fitting also gives directly the parameter $K = 3.0 \times 10^4$ J m^{-3}. This value is used because nearly the same value is obtained by the magnetization-area method [42] applied to our data. The difference between the two results is attributed to the influence of the third free fitting parameter χ_m. The biggest countable volume of the magnetic clusters is now $V = U/K = 230$ nm^3, corresponding to a sphere with a diameter of 7.4 nm (or a cube with a side of 5.9 nm). For the clusters making the highest contribution to magnetization

[5] Gives the mass density interpolation taking into account atomic radii. From a mass density of Hf_2Fe phase being 12 529 kg m^{-3} it follows that 12 000 kg m^{-3} is a good approximation for the mass density of $Hf_{57}Fe_{43}$.

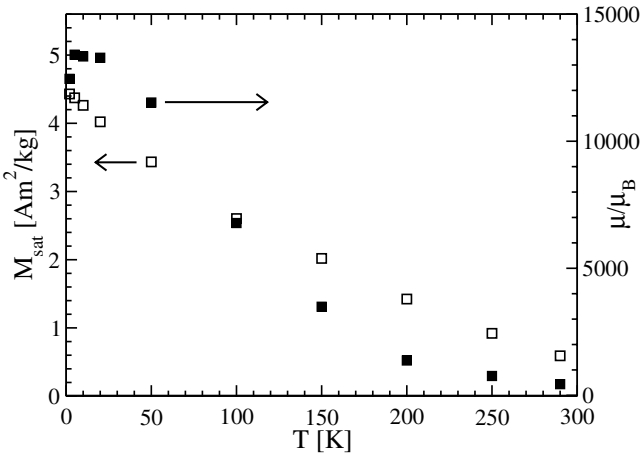

Figure 9. The temperature dependences of the effective magnetic moment of the magnetic clusters μ (■) and saturation of magnetization of clusters M_{sat} (□) derived from $M(H)$ curves.

(maximum at the plot in figure 8) the volume is $V = U/K = 110$ nm^3, corresponding to a sphere with a diameter of 6.1 nm (or a cube with side 4.9 nm). For the cluster with the lowest measured barrier the volume is $V = U/K = 25$ nm^3, corresponding to a sphere with a diameter of 3.6 nm (or a cube with a side of 2.9 nm). With our measurements we can say nothing about smaller clusters. The lower temperatures should be probed for them, or a measuring technique with higher frequencies used. Nevertheless, their contribution to the magnetization is very small. The estimated number of iron atoms based on the volume of the clusters and mass density in magnetic clusters ranges from about 500 to 5000, with a small number of bigger clusters of up to ∼10 000 iron atoms.

The $M(H)$ curve measured at 100 K can be described very well with a rectangular distribution over volumes of clusters. The magnetization of each cluster is given by the Langevin function $L(\mu H/k_{\mathrm{B}}T)$, where $L(x) = 1/\tanh(x) - 1/x$. A flat distribution over magnetic moments is used and the matrix paramagnetic term $\chi_{\mathrm{m}}H$ with known χ_{m} from previous measurement is added taking care about the mass contributions of iron and hafnium. It is not very suitable for fitting a final function to a small number of data points because of the many fitting parameters, but also for a physical reason: the shape of $M(H)$ does not depend very much on the distribution function, but more on the mean value of the magnetic moment, as is well known [29]. Instead, bare plotting shows good agreement between the curve and the measured points using $\mu_{\min} = 800\ \mu_{\mathrm{B}}$ and $\mu_{\max} = 5000\ \mu_{\mathrm{B}}$, that is consistent with number of iron atoms obtained from relaxation analysis. Significantly different values of $\mu_{\min}$ and $\mu_{\max}$ give the significant deviation between the calculated and measured $M(H)$ curves. This points to the consistency of the established picture of the $Hf_{57}Fe_{43}$ system.

The simplification is performed using a superposition of the superparamagnetism of single sized clusters and paramagnetism of the non-magnetic matrix to describe $M(H)$ curves from figure 4. The fitting of

$$M(H) = M_{\mathrm{sat}} L\left(\frac{\mu H}{k_{\mathrm{B}}T}\right) + \chi_{\mathrm{m}} H \tag{5}$$

to the measured $M(H)$ gives the temperature dependence of the effective magnetic moment μ and saturation magnetization of clusters M_{sat} shown in figure 9. The third parameter, the matrix

paramagnetic susceptibility χ_m, stays between 0.12–0.20 J T^{-2} kg^{-1}. It is much bigger than published data for pure hafnium [7, 13] in accordance with the fast increase of paramagnetic susceptibility with iron concentration in Hf–Fe [10] and Zr–Fe [44] systems. Our value of saturation magnetization agrees well with the values for the Hf–Fe system studied in [45] for higher iron concentrations. The deviation of the fitted curves from the measured $M(H)$ in figure 4 becomes more obvious as the temperature decreases. Obviously, the true characteristic magnetic moments below 100 K are smaller than shown in figure 9, and they would correspond more nearly to values obtained from relaxation analysis. Nevertheless, the parameters shown in figure 9 are indicative of the behaviour of the material. The decrease of magnetization saturation with temperature can be understood as destruction of the magnetic ordering of clusters, in agreement with the decrease of magnetic moment.

4.5. Additional remarks

As shown, the presented data are explained very well by the notion of magnetic clusters. This is supported by the investigation of other concentrations of iron in the $Hf_{100-x}Fe_x$ amorphous system, where long range magnetic order for a higher concentration of iron ($x \geqslant 50$) [9] and no magnetic ordering for a lower iron concentration ($x \leqslant 40$) is observed [10]. The iron concentration in $Hf_{57}Fe_{43}$ is well above the percolation threshold, but it seems that magnetic clustering is preferred over long range ordering. The reasons for this should be explored using other experimental techniques. A good starting point might be indirect evidence of non-homogeneous atomic co-ordination in $Hf_{57}Fe_{43}$ metallic glass [46].

Finally, a few remarks may throw more light on the presented system and give impetus for further investigation.

The temperature independence region in $S(T)$ was not observed down to the lowest measured temperatures (1.8 K). The extrapolation of $S(T)$ to zero temperature gives the non-zero relaxation rate. It is still questionable whether such signs of quantum tunnelling of magnetization can be observed in this kind of material at lower temperatures, as has been seen in some random anisotropy magnets [39, 47] and ensembles of magnetic nanoparticles [48]. Theoretical predictions say that magnetization tunnelling could be observable below $\approx$0.1 K [48] in our case.

Additional measurement of $M(H)$ was performed so that every point is taken after the zero-field cooling. The perfect overlap of this $M(H)$ curve with 'single-shot' $M(H)$ measurement shows that every point was measured in equilibrium in both cases, thus excluding spin-glass freezing. Also, the memory effects were investigated in another way [49]. A full hysteresis loop was cycled, then the field was reduced sweeping from the maximum positive field to a negative field somewhere around half of H_{an}, and after that the field was swept from this negative value toward the maximum positive field. The kink at the same positive field around half of H_{an} was not observed. This demonstrates that in $Hf_{57}Fe_{43}$ there is no memory effect connected with a macroscopic number of frustrated symmetric clusters in the spin-glass frame [49].

Hysteresis curves are not shifted after field cooling, excluding further the memory effect. Also, the exchange field between the non-magnetic matrix and the magnetic clusters is negligible. Finite exchange should induce some ordering of the surface layer of the clusters which should couple with their core magnetization, thus shifting the hysteresis loops if measured below the freezing temperature [50]. This is known as the exchange bias. Furthermore, the lack of a shift says that there is no disorder of the surface layer of the clusters which was observed in some magnetic nanoparticle systems [51] and that there are no antiferromagnetic shells around the core of the clusters. It is possible that the magnetic clusters

are below the critical dimension for the onset of the exchange bias [52], or that freezing appears below 2 K.

When considering the relaxation properties, one should bear in mind that it is measured for just one applied magnetic field (0.01 T). From the analysis of blocking temperature it follows that in zero field the characteristic barriers will be two times greater than the barriers when the field is 0.01 T. The influence of magnetic field on the barrier heights will be studied in the future. Furthermore, presented measurements say that high temperature investigation (from 30 K to room temperature or above) would be another interesting topic.

This investigation also gives some hints for a better understanding of magnetism in the similar but more widely investigated Zr–Fe system. It has been thought that below the critical concentration of iron spin-glass behaviour appears [44]. Our work shows that question about the possible blocking of superparamagnetic clusters under some conditions should be raised too.

5. Conclusion

All magnetic measurements performed on binary magnetic/non-magnetic amorphous alloy $Hf_{57}Fe_{43}$ point to its superparamagnetic behaviour and magnetic moment blocking of the clusters. Superparamagnetism is argued for a concentration of iron which is a little below the critical threshold for long range magnetic ordering, so that finite magnetic clusters separated by non-magnetic regions are expected.

ZFC and FC curves, temperature dependent hysteresis loops, slow relaxation of magnetic moment and temperature dependence of magnetic viscosity all show that the magnetic clusters change the direction of their magnetic moment over the magnetic anisotropy barrier by thermal activation. The phenomenological description of the magnetic relaxation using the mentioned quantities and concepts provides a useful link between the experiment and microscopic model. The nanometre sized magnetic clusters in $Hf_{57}Fe_{43}$ alloy are responsible for the observed magnetic processes. Their characteristic volume is estimated roughly to be 25–230 nm^3 using just the magnetic measurements.

Interaction between clusters and the non-magnetic matrix was not observed and the clusters show no memory effects connected to interaction with non-magnetic environment or mutual interaction. Further investigation using magnetometric methods should be performed to describe more precisely the microscopic structure and properties of the magnetic clusters.

The studied system is an excellent potential candidate for investigation of magnetization tunnelling because it is free of surface disorder, exchange bias and other distorting phenomena, at least in the investigated temperature interval. This fundamental quantum process concerns low temperature behaviour and the measurements should be done at much lower temperatures than ours. On the other hand, the high temperature behaviour is interesting for investigating the development of magnetization disorder, which is obviously important for the room-temperature properties of this class of materials.

Acknowledgments

We are grateful to Michael Reissner from the Technical University in Vienna and Davor Čapeta from the University of Zagreb for very valuable discussions. Special thanks is given to Klara Bilić Meštrić for reading the manuscript. This work was supported by the Croatian Ministry of Science, Education and Sports.

References

[1] Hernando A 2003 *Europhys. News* **34** 232
[2] Montgomery C G 1931 *Phys. Rev.* **38** 1782
[3] Bean C P and Livingston J D 1959 *J. Appl. Phys.* **30** 120S
[4] Kittel C 1949 *Rev. Mod. Phys.* **21** 541
[5] Elmore W C 1938 *Phys. Rev.* **54** 1092
[6] Brown W F 1963 *Phys. Rev.* **130** 1677
[7] Crangle J 1991 *Solid State Magnetism* (Princeton, NJ: Van Nostrand-Reinhold) pp 155–73
[8] Bastos C S M, Bahiana M, Nunes W C, Novak M A, Altbir D, Vargas P and Knobel M 2002 *Phys. Rev.* B **66** 214407
[9] Liou S H, Xiao G, Taylor J N and Chien C L 1985 *J. Appl. Phys.* **57** 3535
[10] Ristić R, Zadro K, Pajić D and Babić E 2006 *Int. Conf. on Magnetism (Kyoto, Aug. 2006)*
[11] Pajić D, Zadro K, Ristić R and Babić E 2006 *Int. Conf. on Magnetism (Kyoto, Aug. 2006)*
[12] Révész A, Cziráki Á, Lovas A, Pádár J, Lendvai J and Bakonyi I 2005 *Z. Metallk.* **96** 874
[13] Kriessman C J and McGuire T R 1955 *Phys. Rev.* **98** 936
[14] Bitoh T, Ohba K, Takamatsu M, Shirane T and Chikizawa S 1993 *J. Phys. Soc. Japan* **62** 2583
[15] Fujiki S and Katsura S 1981 *Prog. Theor. Phys.* **58** 1130
[16] Bajpai A and Banarjee A 2001 *J. Phys.: Condens. Matter* **13** 637
[17] Bajpai A and Banerjee A 2000 *Phys. Rev.* B **62** 8996
[18] Wohlfarth E P 1979 *Phys. Lett.* A **70** 489
[19] Chudnovsky E M and Tejada J 1998 *Macroscopic Quantum Tunneling of the Magnetic Moment* (Cambridge: Cambridge University Press) pp 84–126
[20] Bessais L, Ben Jaffel L and Dormann J L 1992 *Phys. Rev.* B **45** 7805
[21] Pajić D, Zadro K, Friščić T, Judaš N and Meštrović E 1999 *Fizika* A **8** 253
[22] Goya G F and Morales M P 2004 *J. Metastable Nanocrystall. Mater.* **20/21** 673
[23] Mydosh J A 1993 *Spin—an Experimental Introduction* (London: Taylor and Francis)
[24] Stoner E C and Wohlfarth E P 1948 *Phil. Trans. R. Soc.* A **240** 599
Stoner E C and Wohlfarth E P 1948 *IEEE Trans. Magn.* **27** 3475
[25] Vértesy G and Tomáš I 1998 *Acta Phys. Slovaca* **48** 663
[26] Tejada J, Zhang X X and Chudnovsky E M 1993 *Phys. Rev.* B **47** 14977
[27] Ribas R, Dieny B, Barbara B and Labarta A 1995 *J. Phys.: Condens. Matter* **7** 3301
[28] Read D A, Moyo T and Hallan G C 1984 *J. Magn. Magn. Mater.* **44** 279
Buschow K J and Kraan A M 1981 *J. Magn. Magn. Mater.* **22** 220
Jayaprakash C and Kirkpatrick C 1980 *Phys. Rev.* B **21** 4072
Denholm D R and Sluckin T J 1993 *Phys. Rev.* B **48** 901
Cresswell A and Paul D I 1990 *J. Appl. Phys.* **67** 398
[29] Nunes W C, Folly W S D, Sinnecker J P and Novak M A 2004 *Phys. Rev.* B **70** 014419
[30] Martínez B, Obradors X, Balcells Ll, Rouanet A and Monty C 1998 *Phys. Rev. Lett.* **80** 181
[31] García-Otero J, García-Bastida A J and Rivas J 1998 *J. Magn. Magn. Mater.* **189** 377
[32] Arnaudas J I, del Moral A and De Groot P A J 1992 *J. Magn. Magn. Mater.* **104–107** 115
[33] Franco V and Conde A 2004 *J. Magn. Magn. Mater.* **278** 28
[34] Chantrell R W, Popplewell J and Charles S W 1980 *J. Magn. Magn. Mater.* **15–18** 1123
[35] St Pierre T G, Gorham N T, Allen P D, Costa-Krämer J L and Rao K V 2001 *Phys. Rev.* B **65** 024436
[36] Iglesias O, Badia F, Labarta A and Balcells Ll 1996 *Z. Phys.* B **100** 173
[37] Aharoni A 1992 *Phys. Rev.* B **46** 5434
[38] Gorham N T, Woodward R C, St Pierre T G, Terris B D and Sun S 2005 *J. Magn. Magn. Mater.* **295** 174
[39] Arnaudas J I, del Moral A, de la Fuente C and de Groot P A J 1993 *Phys. Rev.* B **47** 11924
[40] Pajić D, Zadro K, Vandenberghe R E and Nedkov I 2004 *J. Magn. Magn. Mater.* **281** 353
[41] Tejada J, Ziolo R F and Zhang X X 1996 *Chem. Mater.* **8** 1784
[42] Hadjipanayis G, Sellmyer D J and Brandt B 1981 *Phys. Rev.* B **23** 3349
[43] Bakonyi I 2005 *Acta Mater.* **53** 2509
[44] Hiroyoshi H and Fukamichi K 1982 *J. Appl. Phys.* **53** 2226
[45] Hiroyoshi H, Noguchi K, Fukamichi K and Nakagawa Y 1985 *J. Phys. Soc. Japan* **54** 3554
[46] Gillott L, Guile P N, Cowlam N and Buschow K H J 1983 *Proc. 2nd Int. Conf. on Structure of Non-Crystalline Materials* (London: Taylor and Francis) p 455
[47] Luis F, Bartolomé J, Arnaudas J I, del Moral A and de Groot P A J 1998 *Phys. Rev.* B **58** 9171

[48] Zhang X X, Hernandez J M, Tejada J and Ziolo R F 1996 *Phys. Rev.* B **54** 4101
Awschalom D D, Smyth J F, Grinstein G, DiVincenzo D P and Loss D 1992 *Phys. Rev. Lett.* **68** 3092
[49] Katzgraber H G, Pázmándi F, Pike C R, Liu K, Scalettar R T, Verosub K L and Zimányi G T 2002 *Phys. Rev. Lett.* **89** 257202
[50] Nogués J and Schuller I K 1999 *J. Magn. Magn. Mater.* **192** 203
[51] Zysler R D, Vasquez Mansilla M and Fiorani D 2004 *Eur. Phys. J.* B **41** 171
[52] Dobrynin A N, Levlev D N, Temst K, Lievens P, Margueritat J, Gonzalo J, Afonso C N, Zhou S Q, Vantomme A, Piscopiello E and van Tendeloo G 2005 *Appl. Phys. Lett.* **87** 012501